



Article

Robust Design Optimization for Low-Cost Concrete Box-Girder Bridge

Vicent Penadés-Plà ¹, Tatiana García-Segura ²  and Víctor Yepes ^{1,*} 

¹ Institute of Concrete Science and Technology (ICITECH), Universitat Politècnica de València, 46022 Valencia, Spain; vipepl2@cam.upv.es

² Department of Construction Engineering and Civil Engineering Projects, Universitat Politècnica de València, 46022 Valencia, Spain; tagarse@upv.es

* Correspondence: vyepesp@cst.upv.es

Received: 28 January 2020; Accepted: 8 March 2020; Published: 11 March 2020



Abstract: The design of a structure is generally carried out according to a deterministic approach. However, all structural problems have associated initial uncertain parameters that can differ from the design value. This becomes important when the goal is to reach optimized structures, as a small variation of these initial uncertain parameters can have a big influence on the structural behavior. The objective of robust design optimization is to obtain an optimum design with the lowest possible variation of the objective functions. For this purpose, a probabilistic optimization is necessary to obtain the statistical parameters that represent the mean value and variation of the objective function considered. However, one of the disadvantages of the optimal robust design is its high computational cost. In this paper, robust design optimization is applied to design a continuous prestressed concrete box-girder pedestrian bridge that is optimum in terms of its cost and robust in terms of structural stability. Furthermore, Latin hypercube sampling and the kriging metamodel are used to deal with the high computational cost. Results show that the main variables that control the structural behavior are the depth of the cross-section and compressive strength of the concrete and that a compromise solution between the optimal cost and the robustness of the design can be reached.

Keywords: robust design optimization; RDO; post-tensioned concrete; box-girder bridge; structural optimization; metamodel; kriging

1. Introduction

All structural designs involve variability and uncertainty [1,2]. The initial parameters, the structure dimensions, the mechanical characteristics of the materials, and the loads may differ from the design values [3,4]. Nevertheless, the design of a structure is made using the nominal value, which has a low probability of occurring (for example, the resistance of concrete is the resistance that has a 5% probability of failure). In addition, safety coefficients associated with a given probability of failure are assigned. However, a variation of these initial uncertain parameters can influence the variability of the structural behavior. Structural optimization usually uses a deterministic approach that does not consider the effects of the associated uncertainty [5–13]. This means that the structure has an optimum behavior only under the conditions initially defined, and the response can vary significantly when the values differ from the design values [14,15].

Unlike this approach, robust design has been studied to obtain designs in which the uncertainty of the initial parameters has the lowest possible influence on the objective response. This robust design is reached by a probabilistic optimization. Nowadays, there are two approaches to the optimal probabilistic design of a structure: Reliability-Based Design Optimization (RBDO) [16] and Robust Design Optimization (RDO) [17]. In RBDO, the probability of failure is studied from the variations

of the initial parameters. RDO studies a design that is less sensitive to the variation of the initial parameters. The present paper focuses on the RDO. The concept of robust design was proposed by Taguchi in the 1940s and applied to optimization problems in 1980 [1]. This approach uses the mean and standard deviation to study the variability of the objective response.

The main limitation of RDO is the computational expense because assessing the sensitivity of the objective response of the problem requires a high number of runs [18]. Therefore, it is necessary to find methods that allow carrying out the optimization process more efficiently [4,19,20]. Metamodels allow the generation of a mathematical approximation of the objective response (an objective surface) from the assessment of points within the design space. Once the response surface has been generated, obtaining the value of the objective response given the inputs is much faster. These mathematical approximations or metamodels have already been used to solve RDO process problems [4]. The most widespread metamodels are polynomial regression, artificial neural networks (ANN) and kriging. ANN has been used in different works related to structural engineering [21,22]. However, the kriging model has been demonstrated to be useful to obtain great reliability in the assessment of the response due to its predictive accuracy in non-linear functions [23]. Penadés Plà et al. [24] compared standard heuristic optimization and heuristic optimization based on kriging models, demonstrating that the solutions obtained through optimization based on kriging models are close enough to the solutions obtained through standard heuristic optimization, but with high savings in computational costs.

In the present paper, the robust design methodology is applied to a continuous prestressed concrete box-girder footbridge to obtain a bridge that is optimal in terms of its cost objective function and robust in terms of structural stability. Its structural stability is measured by the variability of the vertical displacement in the middle of the bridge [19]. To this end, Latin hypercube sampling is used to obtain the initial sampling, the kriging model is used to obtain the mathematical approximation to the response, and then the simulated annealing optimization algorithm is used to obtain the robust optimum design. All this will be studied for different uncertain design parameters: the modulus of elasticity, the overload, and the prestressing force.

2. Robust Design Optimization

Robust design studies the variation of the objective response generated by the uncertain initial parameters. Therefore, robust design optimization (RDO) aims to reach the best objective response with the smallest deviation. It implies that the RDO problem is defined as a multi-objective optimization problem in which the objective response is the mean and the standard deviation (Equation (1)).

$$\min\left\{\mu_{F(x,z)}(x_1, x_2, x_3, \dots, x_n), \sigma_{F(x,z)}(x_1, x_2, x_3, \dots, x_n)\right\} \quad (1)$$

where $x_1, x_2, x_3, \dots, x_n$ are the deterministic values of the design variables or the probabilistic function of the uncertain initial parameters.

Commonly, the two objective functions to be minimized in an RDO problem are in conflict. This situation leads to a set of solutions that represent a Pareto frontier. Figure 1 shows an example of the difference between the optimal solution and the robust optimal solution in a design space of one design variable. Solution A is the optimal solution, point B is the most robust solution and point C is the robust optimal solution. It is possible to see that the same variation of the design variable (v) causes a higher variation in the objective function of the solution A (f_A) than it does in the solution C (f_C).

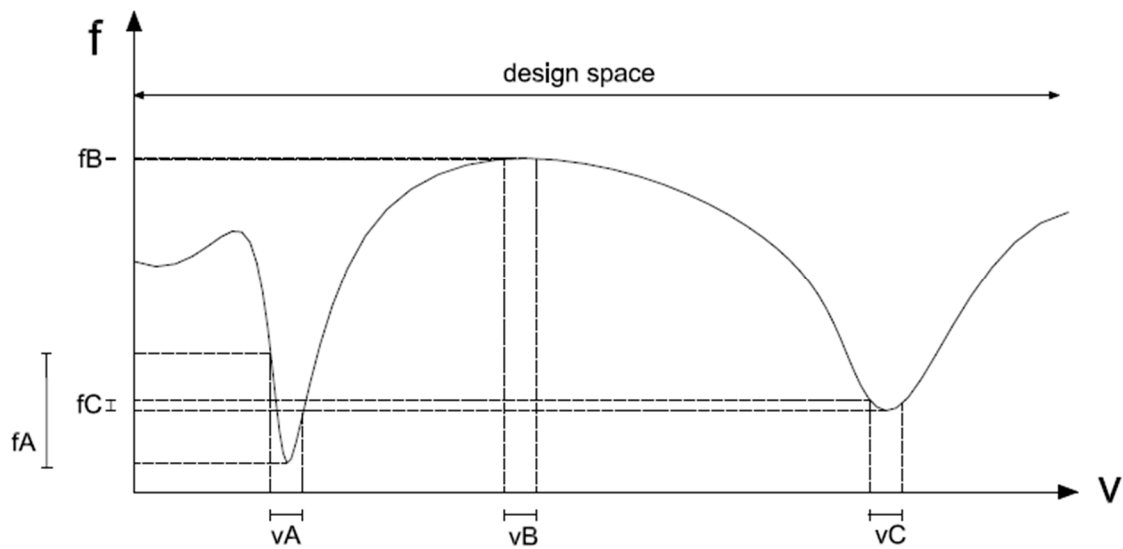


Figure 1. Robust design optimization.

3. Robust Design Optimization Using Metamodels

The main goal of metamodels is to obtain results more efficiently by creating a mathematical approximate model of a detailed simulation model (model of a model). This makes it possible to predict output data (objective response) from input data (variables or design parameters) of the design space. There are three main steps to create a metamodel: (1) obtaining the initial points of the input or sampling data set within the design space (size and position), (2) choosing the method to create the approximate mathematical model, and (3) choosing the fitted model. Each of these three steps can be performed using many different options [25]. In this study, Latin hypercube sampling is used to obtain the initial sampling, the kriging model is used to create the approximate mathematical model, and the search for the Best Linear Unbiased Predictor (BLUP) is used as the fitted model. Then, the mathematical approximation created is used to predict the objective functions according to the initial design variables and parameters. In this way, the optimization can be carried out more efficiently, saving a lot of computational costs, which is important in a probabilistic optimization. In addition, the simulated annealing algorithm is used to perform the optimization. Figure 2 shows a flowchart of the robust design optimization using these characteristics. A more detailed description of this approach can be seen in Penadés-Plà et al. [24].

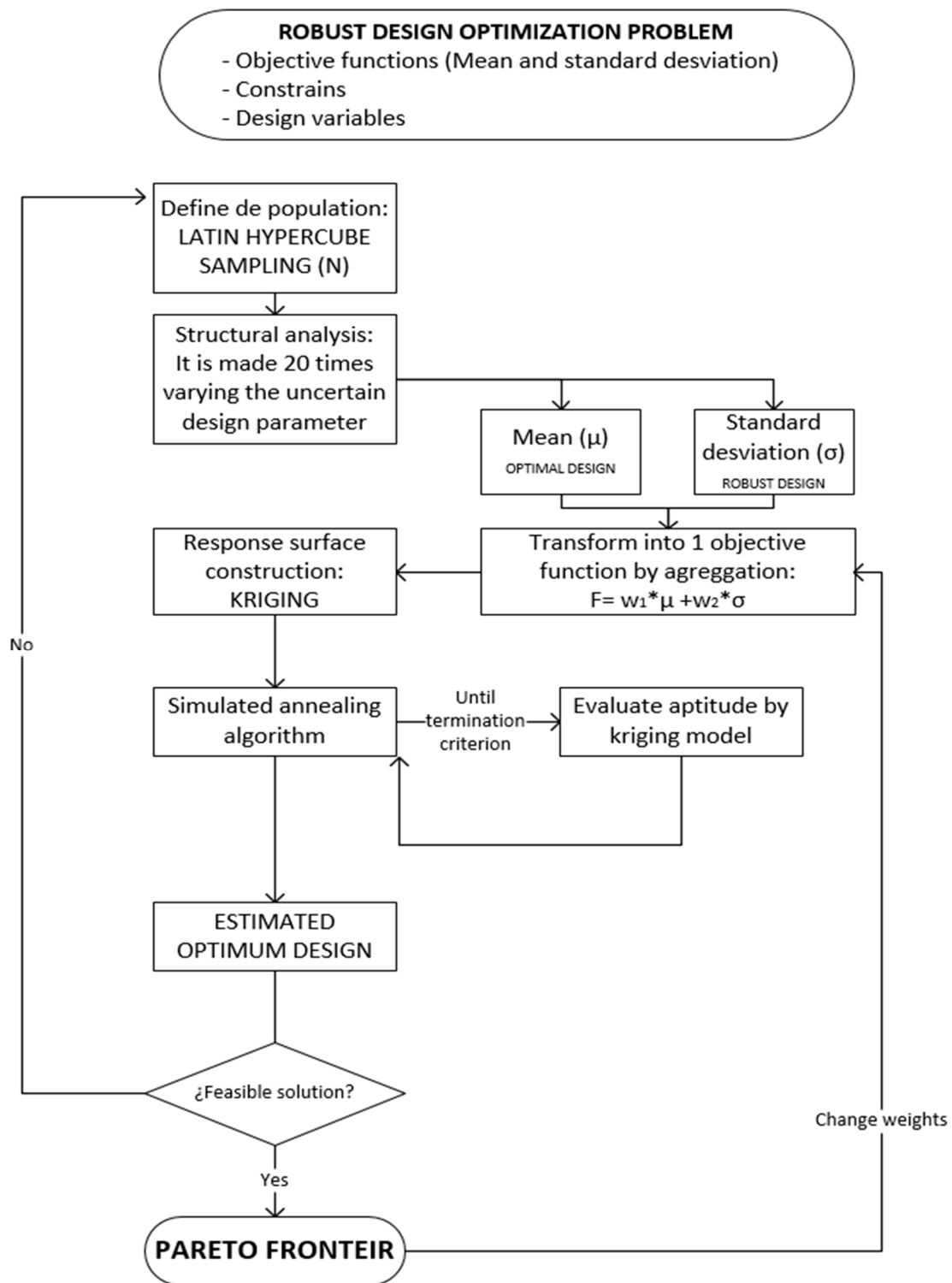


Figure 2. Flow diagram of robust design optimization.

3.1. Latin Hypercube Sampling

McKay et al. proposed in 1979 the Latin hypercube sampling (LHS) [26]. This method is a space-filling type of design of experiments. That means that this type of design of experiment trends to cover all of the design space by the positions of the initial sample points. In this way, local deformation of any area of the design space can be taken into account. For this purpose, a number

N of non-overlapping intervals must first be determined. These intervals divide each range of the design variables (v) into N sections, generating a mesh in the design space with Nv regions. Then, a combination of N random points is generated, so each point is placed in a combination of different intervals of each range of design variables. This guarantees that the initial sampling covers the entire range of each design variable. LHS has been used in several papers, showing its validity for the estimation of metamodel output data [20,27]. For this reason, in the present paper, a uniform distribution of the initial sample points by LHS is employed.

3.2. Kriging

The Kriging metamodel was originally created by Dannie Gerhardus Krige, later much research contributed to its development and finally, Matheron formalized the approach in 1963 [28]. The main idea of the kriging metamodel is that the deterministic response $y(x)$ can be described by

$$y(x) = f(x) + Z(x) \quad (2)$$

where the approximation function is known is called $f(x)$, and $Z(x)$ is an execution of a stochastic process with a mean zero, variance σ^2 and a non-zero covariance. The first term of the equation, $f(x)$, offers a global approach to the design space that is similar to a regression model (Equation (3)). The second term, $Z(x)$, generates local deviations to interpolate the initial sample points using the kriging model (Equation (4)).

$$f(x) = \sum_{i=1}^n \beta_i f_i(x) \quad (3)$$

$$\text{cov}[Z(x_i), Z(x_j)] = \sigma^2 \cdot R(x_i, x_j) \quad (4)$$

where the process variance σ^2 scales the spatial correlation function $R(x_i, x_j)$ between two data points. The Gaussian correlation function (Equation (5)) is widely used in engineering design [29]. It can be defined with a single parameter (θ) that determines the area of influence of the adjacent points [30]. When the sample points have a high correlation, then θ is low, thus $Z(x)$ will be similar throughout the design space. As the θ grows, the closest points will have the greatest correlation, thus $Z(x)$ will vary according to the point in the design space:

$$R(x_i, x_j) = e^{-\sum_{k=1}^m \theta |x_k^i - x_k^j|^2} \quad (5)$$

3.3. The Fitted Model

The search for the Best Linear Unbiased Predictor (BLUP) is used by the formulation of kriging. Simpson et al. [31] have discussed fitting methods for most widely-used metamodels.

3.4. Mean and Variance

The mean (μ) and standard deviation (σ) of the responses of the objectives measure the robust optimum design. These statistical parameters have been obtained for four different levels of uncertainty (10%, 20%, 30%, and 40%). The value of the uncertain initial parameter has been calculated according to a uniform distribution depending on the level of uncertainty. In this way, the mean refers to the optimum design, and the standard variation refers to the robust design.

3.5. Optimization

Simulated annealing (SA) is the heuristic algorithm used to carry out the RDO. This algorithm has been used in a lot of research to solve optimization problems [32,33]. In the present paper, the method of Medina [34] is used to calibrate the initial temperature. This method suggests that the starting temperature is halved when the rate of acceptance is above 40% but doubled when it is below

20%. When a Markov chain ends, the temperature then drops in accordance with a cooling coefficient k based on the equation $T = k \cdot T$. In this study, the calibration showed that the length of the Markov chain of 1000 and a coefficient of cooling of 0.8 are suitable. The algorithm stops after three Markov chains without finding improvements.

4. Problem Design

In this section, the robust design optimization problems proposed are discussed. Section 4.1 describes the structure considered and Section 4.2 defines the characteristics of the problem. Section 4.2 includes the initial uncertain parameters considered and the objective functions studied.

4.1. Description of the Box-Girder Footbridge

The structure is a concrete pedestrian bridge with three continuous spans of 40–50–40 m long. The box-girder cross-section has a uniform width of 3 m, and seven variables define the remaining geometric dimensions of the cross-section (Figure 3): depth (h), web inclination width (d), bottom slab width (b), bottom slab thickness (ei), top slab thickness (es), external cantilever section thickness (ev), and webs slab thickness (ea). The variables are restricted to a range as shown in Table 1. The haunch (c), is determined from the other variables (Equation (6)) as recommended by Schlaich and Scheff [35]. Furthermore, the haunch must also allow space to enclose the ducts in the high and low points. This structure was used to compare the standard heuristic optimization and kriging-based heuristic optimization. In this work, the kriging-based heuristic optimization and RDO are applied to the same structure. More detailed information about this structure can be found in Penadés-Plà et al. [24].

$$t = \max \left\{ \frac{b - 2 \cdot ea}{5}, ei \right\} \tag{6}$$

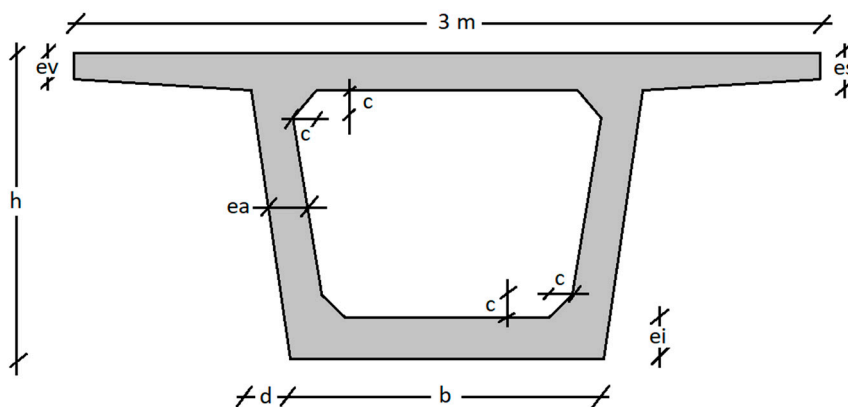


Figure 3. Box-girder cross-section.

Table 1. Main parameters of the analysis.

| Design Variable | Min. Value (m) | Max. Value (m) | Precision (m) |
|------------------------------------------------|----------------|----------------|---------------|
| Depth h | 1.25 | 2.5 | 0.05 |
| Width (b) | 1.2 | 1.8 | 0.05 |
| Inclination width (d) | 0 | 0.4 | 0.05 |
| Top slab thickness (es) | 0.15 | 0.4 | 0.05 |
| External cantilever section thickness (ev) | 0.15 | 0.4 | 0.05 |
| Bottom slab thickness (ei) | 0.15 | 0.4 | 0.05 |
| Webs slab thickness (ea) | 0.3 | 0.6 | 0.05 |

Spanish regulations [36,37] and the Eurocodes [38,39] are used to carry out the structural verification defined by the ultimate and service limit states: bending, vertical shear, longitudinal shear, punching shear, compression and tension stress, torsion, torsion combined with bending and shear, cracking, and vibration. Moreover, compliance with constructability and geometrical criteria must be also checked.

4.2. Description of the Robust Design Optimization Problem

The robust design optimization proposed in this paper is defined by two objective functions: the first one is the mean cost, and the second one is the structural stability represented by the vertical displacement in the middle of the bridge [19]. The statistical parameters for both objective functions are obtained varying the initial uncertain parameter (modulus of elasticity, overload, and prestressing force) according to a uniform distribution with three different levels of uncertainty (10%, 20%, and 30% for the modulus of elasticity and 10%, 20%, 30%, and 40% for the overload and prestressing force). These uncertain parameters were chosen after carrying out a sensitivity analysis of the vertical displacement and selecting the critical parameters.

In this way, the differences between the different Pareto frontiers obtained for each problem can be studied. Therefore, the goal is to obtain the design with the best cost that has the best structural stability for each RDO problem. Equations (7) and (8) correspond to these objective functions assessed.

$$\mu_{COST} = \sum_{i=1,n} e_i \times m_i(x_1, x_2, \dots, x_n) \tag{7}$$

$$\sigma_{VERTICALDISPLACEMENT}(x_1, x_2, x_3, \dots, x_n) \tag{8}$$

where $x_1, x_2, x_3, \dots, x_n$ are the design variables.

The conventional objective function assesses the cost for the construction units taking into account the placement and material used. The BEDEC ITEC database provides unit costs [40]. The compressive strength grade determines the cost of the concrete. The unit costs of the problem are shown in Table 2. The measurements (m_i) relating to the construction units are calculated as defined by the design variables. The variation of the vertical displacement in the middle of the bridge has been obtained according to the standard deviation of 20 different cases varying the initial uncertain parameter. Each one of these vertical displacements has been calculated in accordance with Spanish regulations [36,37] along with the Eurocodes [38,39].

Table 2. Unit cost.

| Unit Measurements | Cost (€) |
|---------------------------------------|----------|
| m ³ of scaffolding | 10.2 |
| m ² of formwork | 33.81 |
| m ³ of lighting | 104.57 |
| kg of steel (B-500-S) | 1.16 |
| kg of post-tensioned steel (Y1860-S7) | 3.40 |
| m ³ of concrete HP-35 | 104.57 |
| m ³ of concrete HP-40 | 109.33 |
| m ³ of concrete HP-45 | 114.10 |
| m ³ of concrete HP-50 | 118.87 |
| m ³ of concrete HP-55 | 123.64 |
| m ³ of concrete HP-60 | 128.41 |
| m ³ of concrete HP-70 | 137.95 |
| m ³ of concrete HP-80 | 147.49 |
| m ³ of concrete HP-90 | 157.02 |
| m ³ of concrete HP-100 | 166.56 |

It is common that a multi-objective optimization problem is transformed into a mono-objective optimization where the objective function is an aggregation function [19] (Equation (9)).

$$\text{Aggregation function} = w_1 \cdot \mu_{\text{COST}} + w_2 \cdot \sigma_{\text{VERTICALDISPLACEMENT}} \tag{9}$$

Here, the mean and the standard deviation are the normalized values of the objective functions, and w_1 and w_2 are weights with values in the range [0,1] such that $w_1 + w_2 = 1$.

In this work, 200 different cases (N) are considered in such a way that w_1 runs from 0 to 1 with increasing $1/N$ and w_2 corresponds to $1-w_1$. In this way, 200 different optimizations are made and all the possible solutions of the Pareto frontier are covered.

5. Results

The results are subdivided into two parts according to the initial uncertain design parameter considered: modulus of elasticity and loads (overload and prestressing force). Each one of these sections provides an initial validation of the kriging surfaces generated, the Pareto frontiers obtained, and some comparisons. For this purpose, 200 points are created to verify the accuracy of the kriging surfaces (validation), and another 200 solutions are obtained from the robust design optimization problems carried out (Pareto frontier). After that, the results will be discussed.

5.1. Variation of Modulus of Elasticity

In this part, the uncertain design parameter studied is the modulus of elasticity. Three different RDO problems are studied. For this purpose, six kriging surfaces are generated depending on the objective function (μ_{cost} and $\sigma_{\text{vertical displacement}}$) and the variability considered of the modulus of elasticity (10%, 20%, and 30%). Table 3 shows the different validations of the different kriging surfaces obtained. The accuracy of the kriging surfaces that predict the mean costs are better than the kriging surfaces that predict the variability of the vertical displacement. The difference between the real and predicted mean value of the cost is lower than 2%, and the difference between the real and predicted standard deviation of the vertical displacement of the middle of the bridge is lower than 5% in all different uncertainties of the modulus of elasticity considered.

Table 3. Validation of the kriging surfaces while varying the modulus of elasticity.

| Uncertainty of E (%) | 10 | 20 | 30 |
|-----------------------------------|-------|-------|-------|
| μ Cost discrepancy | 1.21% | 1.28% | 1.07% |
| σ Displacement discrepancy | 4.63% | 4.75% | 4.03% |

Figure 4 shows the Pareto frontiers for the different uncertainties of the modulus of elasticity considered. This figure represents the mean of the cost against the standard deviation of the vertical displacement of the middle of the bridge. It shows that an increment of the uncertainty of the modulus of elasticity causes a displacement of the Pareto frontier, moving away from the positive ideal point (lowest μ_{cost} and lowest $\sigma_{\text{vertical displacement}}$). This is because the design of the structure should resist all the possible values of the uncertain parameter. Therefore, a higher variation of the initial uncertain parameter imposes greater requirements on the design and an increment of the cost.

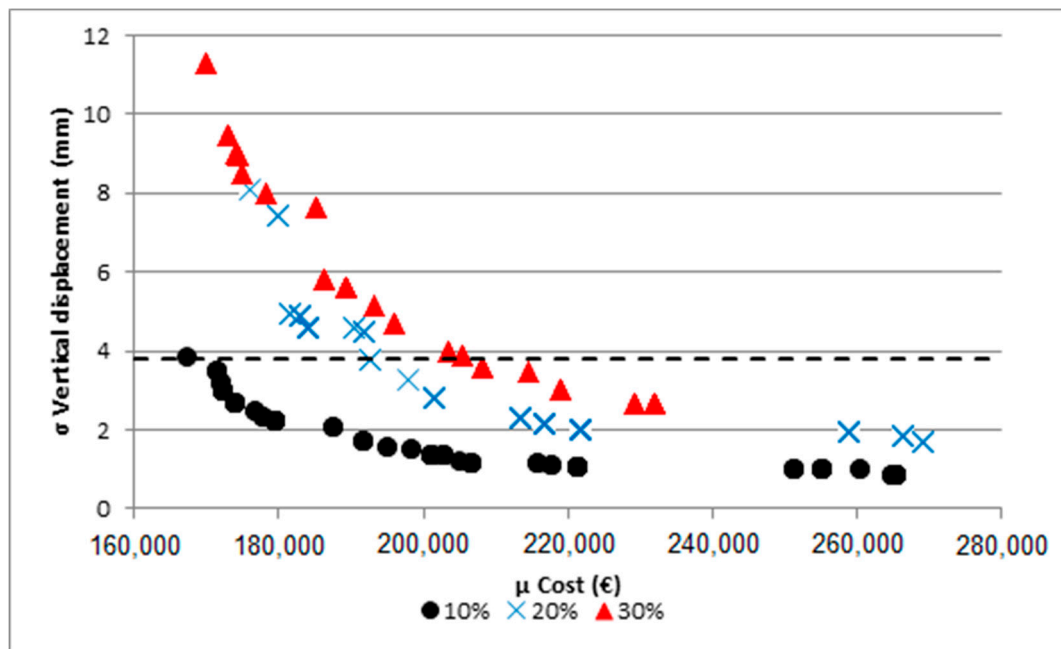


Figure 4. Pareto frontier of modulus of elasticity Robust Design Optimization (RDO) problems.

Table 4 shows a comparison between the designs of the different Pareto frontiers with the same structural behavior. In this case, the reference value taken into account is the standard deviation of the vertical displacement of the cheapest design of the Pareto frontier with the lowest variation of the modulus of elasticity studied. In this way, an imaginary horizontal line will intersect all the Pareto frontiers (dashed line of Figure 4). Solutions S10, S20, and S30 are selected, which correspond to a $\sigma_{\text{vertical displacement}}$ lower than 3.82 mm. It shows that to reach similar structural behavior, the price increases with an increment of the uncertainty of the modulus of elasticity and that the design variables that cause this increment of the price are the depth and f_{ck} . Both are higher for each increment of the variability of the modulus of elasticity.

Table 4. Comparison of design with the same structural behavior in modulus of elasticity RDO problems.

| | b (mm) | h (mm) | d (mm) | e_v (mm) | e_s (mm) | e_a (mm) | e_i (mm) | f_{ck} (MPa) | c (mm) | μ_{cost} (€) | $\sigma_{v,\text{displacement}}$ (mm) |
|-----|--------|--------|--------|------------|------------|------------|------------|----------------|--------|-------------------------|---------------------------------------|
| S10 | 1200 | 1450 | 0 | 150 | 150 | 350 | 225 | 45 | 225 | 167,370.9 | 3.811 |
| S20 | 1200 | 1800 | 125 | 150 | 150 | 350 | 250 | 60 | 250 | 192,570.6 | 3.778 |
| S30 | 1200 | 1950 | 0 | 150 | 150 | 350 | 225 | 80 | 225 | 208,111.9 | 3.548 |

Furthermore, if just one Pareto frontier is studied and three key designs are considered: (A) the optimum or lowest μ_{cost} , (B) the robust optimum or shortest to the positive ideal point, and (C) the most robust or lowest $\sigma_{\text{vertical displacement}}$, the same design variables are affected. For example, Table 5 shows these designs for the Pareto frontier with a 20% variability of the modulus of elasticity. As shown in Table 4, the values of depth and f_{ck} are higher when more robustness is required.

Table 5. Comparison of different designs of the Pareto Frontier with a 20% variation of the modulus of elasticity.

| | b (mm) | h (mm) | d (mm) | e_v (mm) | e_s (mm) | e_a (mm) | e_i (mm) | f_{ck} (MPa) | c (mm) | μ_{cost} (€) | $\sigma_{v,\text{displacement}}$ (mm) |
|---|--------|--------|--------|------------|------------|------------|------------|----------------|--------|-------------------------|---------------------------------------|
| A | 1200 | 1800 | 125 | 150 | 150 | 350 | 250 | 60 | 250 | 192,570.6 | 3.778 |
| B | 1200 | 1900 | 50 | 150 | 150 | 350 | 150 | 80 | 150 | 201,479.9 | 2.794 |
| C | 1800 | 2000 | 200 | 150 | 150 | 350 | 175 | 100 | 220 | 269,128.5 | 1.684 |

5.2. Variation of Loads: Overload and Prestressing Force

In this part, the uncertain design parameters studied are two loads. The first one is the overload due to its high uncertainty, and the second one is the prestressing force to know how the variability influences the behavior of the bridge. The overload is defined according to the IAP-11 [37], which corresponds to 5 kN/m². In this case, due to the higher uncertainty of these parameters, another increment of uncertainty in the loads is considered (40%). Therefore, four RDO problems are studied for each load. For this purpose, eight kriging surfaces are generated for each load depending on the objective function (μ_{cost} and $\sigma_{\text{vertical displacement}}$) and the variability considered of the modulus of elasticity (10%, 20%, 30%, and 40%). In these cases, the results discussed are the same as in the previous subsection. In this way, first, the validations of both loads are discussed (Tables 6 and 7) After that, the Pareto frontiers for each different uncertainty of the design parameter are shown (Figures 5 and 6), and finally some solutions are compared following the same rules as in the previous comparison: the overload (Tables 8 and 9), and the prestressing force (Tables 10 and 11).

Tables 6 and 7 show the different validations of the kriging surfaces obtained. As in the previous cases, the discrepancy of the mean value of the cost is lower than 2% in all cases. However, the discrepancy of the standard deviation of the vertical displacement of the middle of the bridge depends on the variability of the displacement, being higher when the vertical displacement variability is higher and lower when the vertical displacement variability is lower. The results show that when the variability of the overload is lower (10%), the kriging method cannot capture the variability of the displacement accurately. Thus, this uncertainty is not considered.

Table 6. Validation of the kriging surfaces varying the overload.

| Uncertainty of Overload (%) | 10 | 20 | 30 | 40 |
|-----------------------------------|--------|--------|--------|--------|
| μ Cost discrepancy | 1.32% | 1.19% | 1.17% | 1.28% |
| σ Displacement discrepancy | 38.61% | 15.78% | 11.53% | 15.18% |

Table 7. Validation of the kriging surfaces varying the prestressing force.

| Uncertainty of P0 (%) | 10 | 20 | 30 | 40 |
|-----------------------------------|-------|-------|-------|-------|
| μ Cost discrepancy | 1.34% | 1.09% | 1.06% | 1.21% |
| σ Displacement discrepancy | 13.5% | 7.16% | 3.47% | 4% |

Figures 5 and 6 represent the Pareto frontiers for the different variations of the loads. In both cases, the Pareto frontiers have the same behavior as before, moving away from the positive ideal point according to the increment of the uncertainty of the loads. In addition, the comparisons made (Tables 8–11) have similar behavior to the above.

Tables 8 and 10 show a comparison between different designs with the same structural behavior of the different Pareto frontiers. Table 8 corresponds to the RDO problems in which the overload is the uncertain parameter, and the $\sigma_{\text{vertical displacement}}$ of reference corresponds to 2.93 mm (dashed line of Figure 5). Table 9 corresponds to the RDO problems in which the prestressing force is the uncertain parameter, and the $\sigma_{\text{vertical displacement}}$ of reference corresponds to 11.06 mm (dashed line of Figure 6). In both cases, to reach a similar structural behavior the price increases with an increment of the uncertainty of the loads. As well as in the case of the RDO problems in which the modulus of elasticity is the uncertain parameter, the increment of the price is due to the increment of the depth and f_{ck} . The difference is that in the case (where the modulus of elasticity is the uncertain parameter) the depth and the value of f_{ck} increase in each increment of variability, and in the case where the uncertain parameter is the load, the increment of the depth and f_{ck} is not simultaneous. In these cases, a balance between these two design variables is achieved to reach a similar structural behavior. In addition, this increment of depth and f_{ck} is less significant in the case of the overload, due to the low differences among the different uncertainties. The same occurs when the comparison is made between

the optimum or cheapest (A), the robust optimum or shortest to the positive ideal point (B), and the most robust or lowest variation of the vertical displacement (C) (Tables 9 and 11). As above, the key design variables to modify the structural behavior change are the depth and f_{ck} . These variables tend to be higher when higher robustness is required.

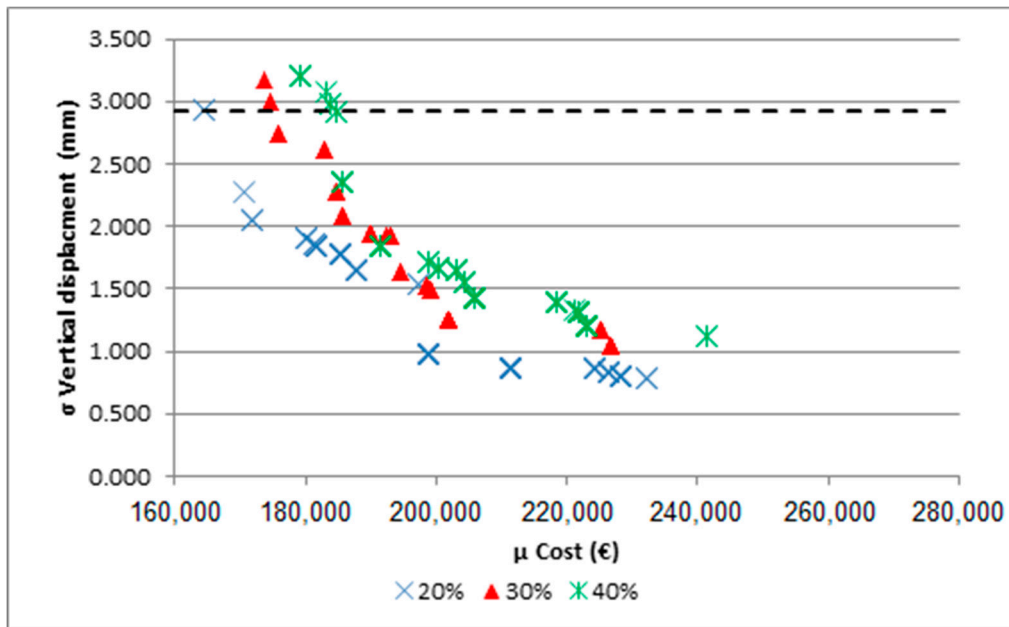


Figure 5. Pareto frontier of overload RDO problems.

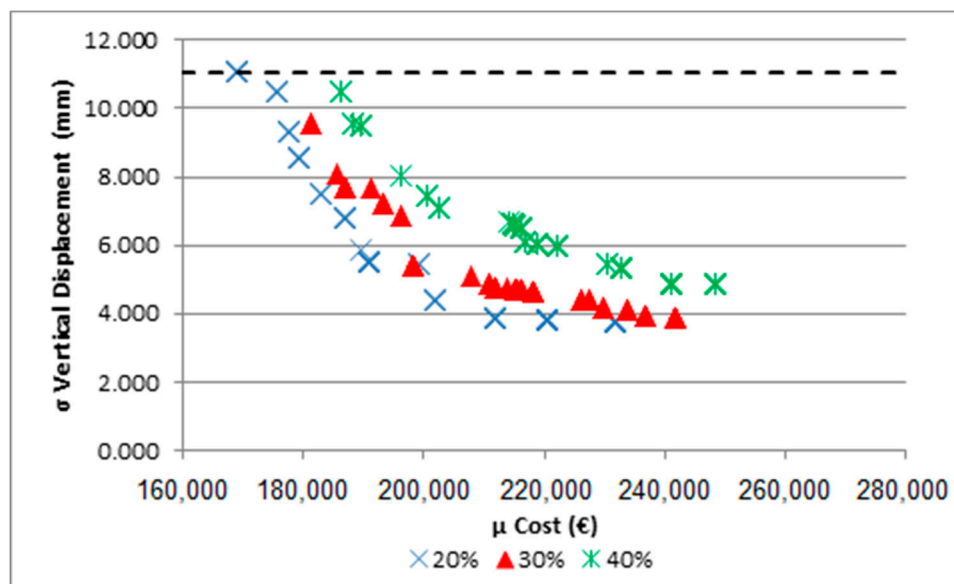


Figure 6. Pareto frontier of prestressing force RDO problems.

Table 8. Comparison of designs with the same structural behavior in overload RDO problems.

| | b (mm) | h (mm) | d (mm) | e_v (mm) | e_s (mm) | e_a (mm) | e_i (mm) | f_{ck} (MPa) | c (mm) | μ_{cost} (€) | $\sigma_{v,displacement}$ (mm) |
|-----|--------|--------|--------|------------|------------|------------|------------|----------------|--------|------------------|--------------------------------|
| S20 | 1200 | 1250 | 0 | 150 | 150 | 350 | 200 | 60 | 200 | 164,594.2 | 2.924 |
| S30 | 1200 | 1250 | 200 | 150 | 150 | 350 | 175 | 70 | 175 | 174,467.1 | 2.991 |
| S40 | 1200 | 1700 | 25 | 175 | 175 | 350 | 250 | 50 | 250 | 184,821.6 | 2.917 |

Table 9. Comparison of different designs of the Pareto Frontier with a 20% variation of the overload.

| | b (mm) | h (mm) | d (mm) | e_v (mm) | e_s (mm) | e_a (mm) | e_i (mm) | f_{ck} (MPa) | c (mm) | μ_{cost} (€) | σ_{v,displacement} (mm) |
|---|------------------|------------------|------------------|------------------------------|------------------------------|------------------------------|------------------------------|--------------------------------|------------------|-----------------------------|-------------------------------------------|
| A | 1200 | 1350 | 100 | 150 | 150 | 350 | 175 | 80 | 175 | 180,240.5 | 1.913 |
| B | 1200 | 1850 | 200 | 175 | 175 | 350 | 225 | 60 | 225 | 198,687.3 | 0.971 |
| C | 1600 | 1800 | 150 | 275 | 275 | 350 | 225 | 70 | 225 | 238,573.8 | 0.753 |

Table 10. Comparison of designs with the same structural behavior in prestressing force RDO problems.

| | b (mm) | h (mm) | d (mm) | e_v (mm) | e_s (mm) | e_a (mm) | e_i (mm) | f_{ck} (MPa) | c (mm) | μ_{cost} (€) | σ_{v,displacement} (mm) |
|-----|------------------|------------------|------------------|------------------------------|------------------------------|------------------------------|------------------------------|--------------------------------|------------------|-----------------------------|-------------------------------------------|
| S20 | 1200 | 1350 | 0 | 150 | 150 | 350 | 200 | 60 | 200 | 168,833.9 | 11.058 |
| S30 | 1200 | 1400 | 200 | 150 | 150 | 350 | 150 | 80 | 150 | 181,276.4 | 9.552 |
| S40 | 1200 | 1750 | 125 | 150 | 150 | 350 | 200 | 55 | 200 | 186,380.7 | 10.497 |

Table 11. Comparison of different designs of the Pareto Frontier with a 20% variation of the prestressing force.

| | b (mm) | h (mm) | d (mm) | e_v (mm) | e_s (mm) | e_a (mm) | e_i (mm) | f_{ck} (MPa) | c (mm) | μ_{cost} (€) | σ_{v,displacement} (mm) |
|---|------------------|------------------|------------------|------------------------------|------------------------------|------------------------------|------------------------------|--------------------------------|------------------|-----------------------------|-------------------------------------------|
| A | 1200 | 1350 | 0 | 150 | 150 | 350 | 200 | 60 | 200 | 168,833.9 | 11.058 |
| B | 1200 | 1650 | 0 | 150 | 150 | 350 | 175 | 80 | 175 | 190,734.7 | 5.510 |
| C | 1300 | 2000 | 0 | 225 | 300 | 350 | 275 | 80 | 275 | 231,832.0 | 3.772 |

6. Conclusions

Currently, the design of structures is made according to a deterministic design. This approach has the result that when the design is optimized according to a conventional objective function, the behavior of the structure is really dependent on the initial values considered. This paper uses a probabilistic approach to consider the variation of the design parameters. In addition, to reduce the large computational cost of the probabilistic optimization, Latin hypercube sampling and kriging metamodels are used. Each point of the Latin hypercube sampling is calculated 20 times varying the initial uncertain parameters (modulus of elasticity, overload, and prestressing force) obtaining the mean of the cost and the standard deviation of the vertical displacement in the middle of the bridge. These values are used to create the kriging surface that predicts the objective response depending on the initial design variables. These surfaces have an error lower than 2% in the mean of the cost for all cases, lower than 5% in the standard deviation of the vertical displacement when the modulus of elasticity is the uncertain parameter, and an accuracy dependent on the value of the vertical displacement when the loads are the uncertain parameters. After that, 200 solutions have been calculated for each case to obtain the different Pareto frontiers.

The Pareto frontiers show that, for all RDO problems, an increment of the uncertainty causes a displacement of the Pareto frontier, moving away from the positive ideal point. That means that to obtain specific robustness when the uncertainty of the parameter is higher, the cost of the design will be higher. In addition, when just one Pareto frontier is taken into account, a more robust design implies an expensive design. In all cases, this increment of the price is due to an increment of two specific design variables: depth (*h*) and *f_{ck}*. Therefore, to obtain a robust design, it is necessary to increment the depth (*h*) and/or *f_{ck}*. However, these Pareto frontiers allow obtaining a compromise design between cost and robustness: the optimum robust design. This solution is the design closest to the positive ideal point.

This work shows that a probabilistic optimization can be carried out to obtain an optimum robust design. Nevertheless, the robust design optimization of complex problems requires a high computational cost. Therefore, the use of metamodels is necessary to carry out probabilistic optimization. In previous works, the computational cost saved and the validity of kriging metamodels were proven. This work shows that the kriging metamodel has an appropriate behavior to carry out the robust design optimization, and therefore can be used to carry out optimization where there is uncertain information.

Author Contributions: This paper represents a result of teamwork. The authors jointly designed the research. V.P.-P. drafted the manuscript. T.G.-S. and V.Y. edited and improved the manuscript until all authors are satisfied with the final version. All authors have read and agreed to the published version of the manuscript.

Funding: This research was funded by the Ministerio de Economía, Ciencia y Competitividad and FEDER funding grant number [BIA2017-85098-R].

Conflicts of Interest: The authors declare no conflict of interest.

References

1. Taguchi, G. *Introduction to Quality Engineering*; Asian Productivity Organisation: Tokyo, Japan, 1986.
2. Phadke, M.S.; Shridhar, M. *Quality Engineering Using Robust Design*; Prentice Hall: Upper Saddle River, NJ, USA, 1989.
3. Fowlkes, W.Y.; Creveling, C.M. *Engineering Method for Robust Product Design*; Addison-Wesley Publishing Company: Boston, MA, USA, 1995.
4. Lee, K.-H.; Kang, D.-H. A robust optimization using the statistics based on kriging metamodel. *J. Mech. Sci. Technol.* **2006**, *20*, 1169–1182. [[CrossRef](#)]
5. Carbonell, A.; González-Vidosa, F.; Yepes, V. Design of reinforced concrete road vaults by heuristic optimization. *Adv. Eng. Softw.* **2011**, *42*, 151–159. [[CrossRef](#)]
6. Ahsan, R.; Rana, S.; Nurul Ghani, S. Cost optimum design of posttensioned I-girder bridge using global optimization algorithm. *J. Struct. Eng.* **2012**, *138*, 272–283. [[CrossRef](#)]
7. García-Segura, T.; Yepes, V.; Martí, J.V.; Alcalá, J. Optimization of concrete I-beams using a new hybrid glowworm swarm algorithm. *Lat. Am. J. Solids Struct.* **2014**, *11*, 1190–1205. [[CrossRef](#)]
8. Pnevmatikos, N.G.; Thomos, G.T. Stochastic structural control under earthquake excitations. *Struct. Control Health Monit.* **2014**, *21*, 620–633. [[CrossRef](#)]
9. García-Segura, T.; Yepes, V. Multiobjective optimization of post-tensioned concrete box-girder road bridges considering cost, CO₂ emissions, and safety. *Eng. Struct.* **2016**, *125*, 325–336. [[CrossRef](#)]
10. Martí, J.V.; García-Segura, T.; Yepes, V. Structural design of precast-prestressed concrete U-beam road bridges based on embodied energy. *J. Clean. Prod.* **2016**, *120*, 231–240. [[CrossRef](#)]
11. Yepes, V.; Martí, J.V.; García-Segura, T.; González-Vidosa, F. Heuristics in optimal detailed design of precast road bridges. *Arch. Civ. Mech. Eng.* **2017**, *17*, 738–749. [[CrossRef](#)]
12. Sun, X.; Fu, H.; Zeng, J. Robust approximate optimality conditions for uncertain nonsmooth optimization with Infinite number of constraints. *Mathematics* **2018**, *7*, 12. [[CrossRef](#)]
13. Rodriguez-Gonzalez, P.T.; Rico-Ramirez, V.; Rico-Martinez, R.; Diwekar, U.M. A new approach to solving stochastic optimal control problems. *Mathematics* **2019**, *7*, 1207. [[CrossRef](#)]
14. Moayyeri, N.; Gharehbaghi, S.; Plevris, V. Cost-based optimum design of reinforced concrete retaining walls considering different methods of bearing capacity computation. *Mathematics* **2019**, *7*, 1232. [[CrossRef](#)]
15. Sierra, L.A.; Yepes, V.; García-Segura, T.; Pellicer, E. Bayesian network method for decision-making about the social sustainability of infrastructure projects. *J. Clean. Prod.* **2014**, *176*, 521–534. [[CrossRef](#)]
16. Valdebenito, M.A.; Schuëller, G.I. A survey on approaches for reliability-based optimization. *Struct. Multidiscip. Optim.* **2010**, *42*, 645–663. [[CrossRef](#)]
17. Doltsinis, I.; Kang, Z. Robust design of structures using optimization methods. *Comput. Methods Appl. Mech. Eng.* **2004**, *193*, 2221–2237. [[CrossRef](#)]
18. Simpson, T.W.; Booker, A.J.; Ghosh, D.; Giunta, A.A.; Koch, P.N.; Yang, R.-J. Approximation methods in multidisciplinary analysis and optimization: A panel discussion. *Struct. Multidiscip. Optim.* **2004**, *27*, 302–313. [[CrossRef](#)]
19. Martínez-Frutos, J.; Martí, P. Diseño óptimo robusto utilizando modelos Kriging: Aplicación al diseño óptimo robusto de estructuras articuladas. *Rev. Int. Métodos Numéricos para Cálculo y Diseño Ing.* **2014**, *30*, 97–105. [[CrossRef](#)]
20. Jin, R.; Chen, W.; Simpson, T.W. Comparative studies of metamodeling techniques under multiple modeling criteria. *Struct. Multidiscip. Optim.* **2001**, *23*, 1–13. [[CrossRef](#)]
21. Martí-Vargas, J.R.; Ferri, F.J.; Yepes, V. Prediction of the transfer length of prestressing strands with neural networks. *Comput. Concr.* **2013**, *12*, 187–209. [[CrossRef](#)]

22. Salehi, H.; Burgueno, R. Emerging artificial intelligence methods in structural engineering. *Eng. Struct.* **2018**, *171*, 170–189. [[CrossRef](#)]
23. Jin, R.; Du, X.; Chen, W. The use of metamodeling techniques for optimization under uncertainty. *Struct. Multidiscip. Optim.* **2003**, *25*, 99–116. [[CrossRef](#)]
24. Penadés-Plà, V.; García-Segura, T.; Yepes, V. Accelerated optimization method for low-embodied energy concrete box-girder bridge design. *Eng. Struct.* **2019**, *179*, 556–565. [[CrossRef](#)]
25. Barton, R.R.; Meckesheimer, M. Metamodel-based simulation optimization. *Handb. Oper. Res. Manag. Sci.* **2006**, *13*, 535–574.
26. McKay, M.D.; Beckman, R.J.; Conover, W.J. Comparison of three methods for selecting values of input variables in the analysis of output from a computer code. *Technometrics* **1979**, *21*, 239–245.
27. Chuang, C.H.; Yang, R.J.; Li, G.; Mallela, K.; Pothuraju, P. Multidisciplinary design optimization on vehicle tailor rolled blank design. *Struct. Multidiscip. Optim.* **2008**, *35*, 551–560. [[CrossRef](#)]
28. Matheron, G. Principles of geostatistics. *Econ. Geol.* **1963**, *58*, 1246–1266. [[CrossRef](#)]
29. Simpson, T.W.; Mauery, T.M.; Korte, J.; Mistree, F. Kriging models for global approximation in simulation-based multidisciplinary design optimization. *AIAA J.* **2001**, *39*, 2233–2241. [[CrossRef](#)]
30. Forrester, A.I.J.; Keane, A.J. Recent advances in surrogate-based optimization. *Prog. Aerosp. Sci.* **2009**, *45*, 50–79. [[CrossRef](#)]
31. Simpson, T.W.; Poplinski, J.D.; Koch, P.N.; Allen, J.K. Metamodels for computer-based engineering design: Survey and recommendations. *Eng. Comput.* **2001**, *17*, 129–150. [[CrossRef](#)]
32. Camp, C.V.; Huq, F. CO₂ and cost optimization of reinforced concrete frames using a big bang-big crunch algorithm. *Eng. Struct.* **2013**, *48*, 363–372. [[CrossRef](#)]
33. Martí, J.V.; González-Vidosa, F.; Yepes, V.; Alcalá, J. Design of prestressed concrete precast road bridges with hybrid simulated annealing. *Eng. Struct.* **2013**, *48*, 342–352. [[CrossRef](#)]
34. Medina, J.R. Estimation of incident and reflected waves using simulated annealing. *J. Watery Port Coast. Ocean Eng* **2001**, *127*, 213–221. [[CrossRef](#)]
35. Schlaich, J.; Scheef, H. *Concrete Box-Girder Bridges*; International Association for Bridge and Structural Engineering: Zürich, Switzerland, 1982.
36. Ministerio de Fomento. *EHE-08: Code on Structural Concrete*; Ministerio de Fomento: Madrid, Spain, 2008.
37. Ministerio de Fomento. *IAP-11: Code on the Actions for the Design of Road Bridges*; Ministerio de Fomento: Madrid, Spain, 2011.
38. European Committee for Standardization. *EN 1001-2: Eurocode 1: Actions on Structures-Part 2: Traffic Loads Bridges*; European Committee for Standardization: Brussels, Belgium, 2003.
39. European Committee for Standardisation. *EN1992-2: Eurocode 2: Design of Concrete Structures-Part 2: Concrete Bridge-Design and Detailing Rules*; European Committee for Standardisation: Brussels, Belgium, 2005.
40. Catalonia Institute of Construction Technology. *BEDEC PR/PCT ITEC Material Database*; Catalonia Institute of Construction Technology: Barcelona, Spain, 2016.

